Mechanically modulated spin-orbit couplings in oligopeptides

Juan Daniel Torres [1], Raúl Hidalgo-Sacoto [1], Solmar Varela [2,1,*] and Ernesto Medina [1,3,4,†]

[1] *Yachay Tech University, School of Physical Sciences & Nanotechnology, 100119-Urcuquí, Ecuador*

[2] *Yachay Tech University, School of Chemical Sciences & Engineering, 100119-Urcuquí, Ecuador*

[3] *Simon A. Levin Mathematical, Computational and Modeling Sciences Center, Arizona State University, P.O. Box 873901, Tempe, Arizona 85287-3901, USA*

[4] *Centro de Física, Instituto Venezolano de Investigaciones Científicas, Caracas, Venezuela*

(Received 4 March 2020; revised 20 May 2020; accepted 29 June 2020; published 20 July 2020)

Recently experiments have shown very significant spin activity in biological molecules such as DNA, proteins, oligopeptides, and aminoacids. Such molecules have in common their chiral structure, time reversal symmetry and the absence of magnetic exchange interactions. The spin activity is then assumed to be due to either the intrinsic spin-orbit (SO) interaction or SO coupled to the presence of strong local sources of electric fields. Here we derive an analytical tight-binding Hamiltonian model for oligopeptides that contemplates both intrinsic SO and Rashba interaction induced by hydrogen bonding. We use a lowest order perturbation theory band-folding scheme and derive the reciprocal space intrinsic and Rashba type Hamiltonian terms to evaluate the spin activity of the oligopeptide and its dependence on molecule uniaxial deformations. SO strengths in the tens of meV are found and explicit spin active deformation potentials. We find a rich interplay between responses to deformations both to enhance and diminish SO strength that allow for experimental testing of the orbital model. Qualitative consistency with recent experiments shows the role of hydrogen bonding in spin activity. Hydrogen bonding as the source of spin activity further enhances, coupled to chirality, the ubiquity of spin effects that may be pervasive and functional in biological molecular structures.

DOI: 10.1103/PhysRevB.102.035426

I. INTRODUCTION

There has been considerable interest recently in the electron spin polarizing ability of biological chiral molecules such as DNA, proteins, oligopeptides, and aminoacids [1–5]. The effect known as chiral-induced spin selectivity (CISS) is impressive since the electron polarizations achieved, both for self-assembled monolayers and single molecule setups, exceeds those of ferromagnets [6]. The qualitative explanation for spin activity, in the absence of a time reversal symmetry breaking interactions, has been suggested to be due to the atomic spin-orbit coupling [7,8]. Although the small size of such an interaction has encouraged invoking sources such as inelastic effects [9–11], recent works have shown that tunneling alone can exponentiate the small spin-orbit values to yield very high polarizations [12].

Analytical tight-binding modeling has proven very powerful to understand the qualitatively different features of low dimensional systems. An emblematic example is the discovery of topological insulators [13] and the integer quantum hall effects without magnetic fields [14]. In the context of the CISS effect, a recent model [15] described the spin activity of DNA on the basis of a tight-binding (TB) model that assumes mobile electrons on the π orbitals of the bases and the spin-orbit coupling (SOC) due to the intra-atomic interactions of C, O, and N. The resulting model yields a consistent picture of how a time reversal symmetric Hamiltonian can result in spin polarization. A more recent analytical TB model has also described spin-polarizing transport features of Helicene [16].

While attempting to assess the dominant player in electron spin transport effects on large chiral molecules, an opportunity arises to validate the orbital model using mechanical deformations [17]. The spin polarization response hints at the orbital participation involved in determining the SOC strength [18,19]. One can then also perform transport calculations and determine the behavior of a finite system including details of the coupling to reservoir [20].

In this work, we derive an analytical tight-binding Hamiltonian model for oligopeptides that assumes that the basic ingredients are (i) the atomic SO interaction from double bonded (orbital) oxygen atoms, in the carboxyl units, provide transport electrons, (ii) the Stark interaction matrix element between the p_z orbital and the oxygen s orbital is produced by the hydrogen bond polarization, and (iii) overlaps between nearest neighbor oxygen orbitals [21]. The manifestations of these ingredients through a mechanical probe will be a specially compelling verification of the source the electric field feeding the SOC and determining its magnitude. The case for oligopeptides [17], because of the arrangement of the hydrogen bonds, is very different from that of DNA [19] and should yield opposite effects on stretching. Finally, there are already experimental results for CISS on oligopeptides that will serve as an experimental check.

The paper is organized as follows: in Sec. II we first introduce the full TB model of the oligopeptide including both the Stark and the SOC. Then we use band folding

*svarela@yachaytech.edu.ec

†emedina@yachaytech.edu.ec

to reduce an 8×8 space encompasing the orbital space to a 2×2 effective space involving one effective p_z per site. Thus we derive the resulting Rashba and intrinsic SOC's and energy corrections. We find closed form expressions for dependences of the interactions on the geometry of the molecule and the type of amino-acid units. There arise four different SOC terms: two associated to the Rashba interaction and two to the intrinsic coupling. In Sec. III we obtain the Hamiltonian in reciprocal space by way of a Bloch expansion. In Sec. IV we show the analysis of the behavior of the SOC magnitudes under deformations. The interplay between these spin active interactions yield opposite responses to the longitudinal mechanical deformations, with predominance of the SO enhanced stretching. Furthermore, the Rashba coupling, depending on the polarization of the hydrogen bond, yields additional enhanced SO due to stretching as reported experimentally for oligopeptides [17]. These results point to the role of the atomic SO and hydrogen bonding in the spin activity of biological molecules. Finally, in Sec. V we offer summary and conclusions.

II. TIGHT-BINDING MODEL

Consider a helix as shown in Fig. 1. Each atom is described by a set of $\{s, p_x, p_y, p_z\}$ orbitals associated with valence oligopetide constituents such as C, N, O. The mobile electrons are assumed to be provided with the double bonded oxygen [21] (carboxyl group) attached by hydrogen bonding [see Fig. 1(a)] to the amine group in the oligopeptide. The high polarization of the hydrogen bonds produce local electric fields on carboxyl group. The hydrogen bonds connect consecutive helix turns as shown by dashed lines in Fig. 1(a). Such bonds have a small tilting due to a small nonperiodicity of real structures [22], which we capture in our model. The π structure of the double-bonded oxygen is accounted for by the p_z orbitals in the radial direction [see Fig. 1(b)] akin to the structure of a single walled nanotube. The backbone of the molecule is bonded through the σ structure, *i.e.* $\{s, p_x, p_y\}$ *orbitals*, that lie tangentially to the oligopeptide structure. These bonds mediate alternate electron transfer paths between p_z orbitals that are small compared to the direct $p_z - p_z$ transfer or kinetic term, such that they are omitted in our model. The axis of the chain is considered along the *Y*axis with a set of orbitals on sites ι, such that $\iota = 1, ..., N$. The position vector $\mathbf{R}_\iota$ in the fixed or global coordinate system (*XYZ*) describes points on a cylinder and is written as

$$\mathbf{R}_\iota = r\cos[(\iota-1)\Delta\varphi]\mathbf{e_Z} + r\sin[(\iota-1)\Delta\varphi]\mathbf{e_X} + h\frac{(\iota-1)\Delta\varphi}{2\pi}\mathbf{e_Y}, \quad (1)$$

where r is the radius of the helix, h is the pitch, and $\Delta\varphi$ represents the angle between the positions of two consecutive sites. The vector that connects two sites ι and $\jmath$ of the helix is $\mathbf{R}_{\jmath\iota} = \mathbf{R}_\jmath - \mathbf{R}_\iota$. Structural parameters used [22] to describe a real oligopeptide can be found in Table III in Appendix B.

Electrons are well coupled along the helical structure (as opposed to the coupling from one turn of the helix to the next) and couplings between π and σ structures are included. The

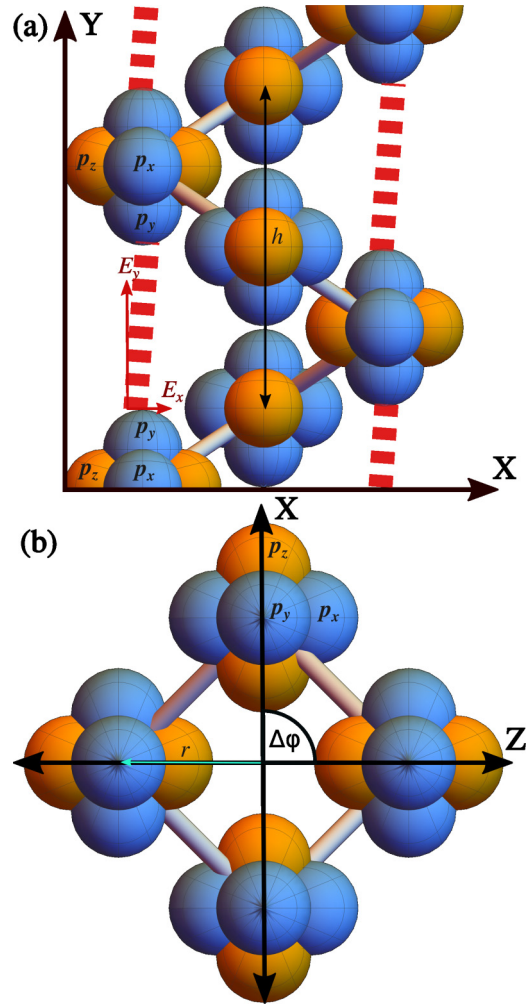

FIG. 1. (a) Front view of the helical oligopeptide in the XY-plane. The pitch of the helix is indicated as h and labels for each p orbital are shown. The internal electric field caused by the hydrogen bond and the component along each direction are shown in red. (b) Top view of the helical oligopeptide in the XZ plane where r represents the radius of the helix, and $\Delta\varphi$ is the angle between consecutive amino acids.

full Hamiltonian of the system can be written in the form

$$H = H_K + H_{SO} + H_S, \quad (2)$$

where H_K is the kinetic term or the bare Slater-Koster (SK) overlaps, H_{SO} include the SO interactions, and H_S is the Stark interaction resulting from electric dipoles (hydrogen bonding) in the molecule.

A. Stark interaction and hydrogen bonding

In a helical peptide, the hydrogen bonds between the amino and carboxyl groups stabilize the helical structure [23]. As shown in Refs. [18,24], the near field electrostatics of the bond yield among the highest electric field one finds in a molecules that goes unscreened. These electrostatic fields, have been proposed to generate local interactions that open new transport channels. In the model, the Stark interaction associated with hydrogen bond polarization couples s with

TABLE I. SO matrix elements between p orbitals in the local coordinate system.

	$\|p_x\rangle$	$\|p_y\rangle$	$\|p_z\rangle$
$\langle p_x\|$	0	$-iz_p\mathbf{s_z}$	$iz_p\mathbf{s_y}$
$\langle p_y\|$	$iz_p\mathbf{s_z}$	0	$-iz_p\mathbf{s_x}$
$\langle p_z\|$	$-iz_p\mathbf{s_y}$	$iz_p\mathbf{s_x}$	0

p orbitals on the double bonded oxygen of the carboxyl group along the direction of the dipole field in the form $H_S = -e\mathbf{E}\cdot\mathbf{r}$ where $\mathbf{E}$ is the electric field (see Ref. [18]), $\mathbf{r} = r(\sin\theta\sin\varphi, \cos\theta, \sin\theta\cos\varphi)$ is the vector position in spherical coordinates, θ being the angle with Y axis, and e is the electron charge. Then, in local coordinates, we have

$$H_S = -er(E_x \sin\theta\cos\varphi + E_y\cos\theta), \tag{3}$$

where $E_{x,y}$ represents the components of the electric field in the indicated directions (red arrows in Fig. 1). The source of the electric field along x and y was obtained from Ref. [18] where the electric field was computed accounting for the local dipole field of hydrogen bonding.

In general, the hydrogen bond direction has a component both along the x and y directions. However, the component along the x direction is much smaller than the y component, since the bond is essentially in the $Y = y$ direction. Then, consider ξ_{sx} and ξ_{sy}, where these are given by

$$\xi_{sx} = \langle s|H_S|p_x\rangle, \qquad \xi_{sy} = \langle s|H_S|p_y\rangle. \tag{4}$$

In the case of mechanical deformation, higher order terms may be relevant when the helix is stretched.

B. Spin-orbit interactions

The SO interaction has been well described by tight-binding treatments in the context of low dimensional systems [15,25–27]. The atomic SO interaction couples the spin of the electron to the internal electric field of the nuclei. The SO Hamiltonian is

$$\begin{aligned} H_{SO} &= \frac{e}{2m_o^2c^2}(\nabla V \times \mathbf{p})\cdot\mathbf{S}, \\ &= \Gamma\mathbf{L}\cdot\mathbf{S}, \end{aligned} \tag{5}$$

where V is electrical potential of the nuclei as seen by valence electrons of the orbital basis, m_o is the rest electron mass, e is the charge of the electron, c is the speed of light, $\mathbf{S}$ and $\mathbf{L}$ are the spin and orbital angular momentum operators, respectively. The SO matrix elements couple the basis p orbitals as shown in Table I, where $z_p = \Gamma/2$ is the magnitude of the SO interaction for p orbitals and s_j are the Pauli matrices in the rotating coordinate system. The rotated spin operators, i.e., the spin operators in the local frame, are

$$\begin{aligned} \mathbf{s}_x &= -\sin(\varphi_i)\sigma_x + \cos(\varphi_i)\sigma_z, \\ \mathbf{s}_y &= \sigma_y, \\ \mathbf{s}_z &= \cos(\varphi_i)\sigma_x + \sin(\varphi_i)\sigma_z. \end{aligned} \tag{6}$$

There are two relevant SO interactions that lead to different spin active processes. The first is the intrinsic SO interaction,

TABLE II. The matrix elements of the full Hamiltonian in the local coordinate system. The π and σ spaces are the diagonal components while the off diagonal correspond to T and $T^\dagger$ of Eq. (11).

	$\|p_z\rangle_i$	$\|p_z\rangle_j$	$\|s\rangle_i$	$\|p_x\rangle_i$	$\|p_y\rangle_i$	$\|s\rangle_j$	$\|p_x\rangle_j$	$\|p_y\rangle_j$
$\langle p_z\|_i$	ϵ_p^π	V_z	0	$-iz_p\mathbf{s_y}$	$iz_p\mathbf{s_x}$	V_s	V_x	V_y
$\langle p_z\|_j$	V_z	ϵ_p^π	V_s	$-V_x$	$-V_y$	0	$-iz_p\mathbf{s_y}$	$iz_p\mathbf{s_x}$
$\langle s\|_i$	0	V_s	ϵ_s	ξ_{sx}	ξ_{sy}	0	0	0
$\langle p_x\|_i$	$iz_p\mathbf{s_y}$	$-V_x$	ξ_{sx}	ϵ_p^σ	0	0	0	0
$\langle p_y\|_i$	$-iz_p\mathbf{s_x}$	$-V_y$	ξ_{sy}	0	ϵ_p^σ	0	0	0
$\langle s\|_j$	V_s	0	0	0	0	ϵ_s	ξ_{sx}	ξ_{sy}
$\langle p_x\|_j$	V_x	$iz_p\mathbf{s_y}$	0	0	0	ξ_{sx}	ϵ_p^σ	0
$\langle p_y\|_j$	V_y	$-iz_p\mathbf{s_x}$	0	0	0	ξ_{sy}	0	ϵ_p^σ

which is the pure matrix element between atomic orbitals, i.e., H_{SO}. This interaction can be understood as a transport process in the π structure with intermediate steps in the σ structure. The paths of first order in SO coupling are

$$p_z^\imath \to E_{zx}^{\imath\jmath} \to p_x^\jmath \to z_p \to p_z^\jmath, \tag{7}$$

$$p_z^\imath \to E_{zy}^{\imath\jmath} \to p_y^\jmath \to z_p \to p_z^\jmath, \tag{8}$$

where the SK overlaps $E_{\mu\mu'}^{\imath\jmath}$ between an orbital μ on $\imath$ site and orbital μ' on site $\jmath$, are defined in Appendix B. The second type of SO interaction is possible when there is Stark interaction. The Rashba SO interaction arises as a combination of both the Stark interaction and the bare SO coupling. The Stark interaction has been argued to be the strongest source of electric fields in molecules outside the vicinity of the nucleus [18] because of the presence of hydrogen bond polarization in the near field [24]. The paths of a first order Rashba process are

$$p_z^\imath \to E_{zs}^{\imath\jmath} \to p_s^\jmath \to \xi_{sx} \to p_x^\jmath \to z_p \to p_z^\jmath, \tag{9}$$

$$p_z^\imath \to E_{zs}^{\imath\jmath} \to p_s^\jmath \to \xi_{sy} \to p_y^\jmath \to z_p \to p_z^\jmath. \tag{10}$$

Geometrical details of the problem determine the effective SO magnitudes resulting from the interplay between different first order transport processes, e.g., interference between Eqs. (9) and (10).

C. Effective Hamiltonian

The Hamiltonian of Eq. (2) in the basis of atomic orbitals can be written as

$$H = \begin{pmatrix} H_\pi & T \\ T^\dagger & H_\sigma \end{pmatrix}, \tag{11}$$

where H_π and H_σ are the structural Hamiltonians and T correspond to the connection between π and σ spaces. In Table II, all the matrix elements of the full Hamiltonian are written explicitly. Here, the SK overlaps are represented by V_s, V_x, V_y, and V_z are calculated using the Harrison formula [28] (see Appendixes B and A), ϵ_p^σ is the site energy for the bonded orbitals p_x and p_y, ϵ_p^π is the site energy of the orbital p_z, and ϵ_s is the energy of the orbital s.

The goal is to obtain an effective Hamiltonian that describes the π space including the physics of the σ space as

a perturbation. For this purpose, we use an energy independent perturbative partitioning approach developed by Löwdin [29–32]. The band folding (BF) method (see Appendix C) is used to obtain an effective Hamiltonian using matrix perturbation theory. It is a canonical transformation in the same sense of the Foldy-Wouthuysen transformation [33] maintaining only first order corrections. The effective Hamiltonian for the π structure is

$$\mathcal{H} \approx H_\pi - T H_\sigma^{-1} T^\dagger. \tag{12}$$

No additional corrections, to the same order, arise from wavefunction normalization [34]. Then, one simplifies the problem from 8×8, in orbital and site space, to 2×2. Spin active terms are written implicit. Using Eq. (12) and the corresponding matrices for the subspaces shown in Table II, we obtain the effective Hamiltonian

$$\mathcal{H} = \begin{pmatrix} \epsilon_\pi & V_z - i((\boldsymbol{\alpha}+\boldsymbol{\lambda})\times \mathbf{s})_z \\ V_z + i((\boldsymbol{\alpha}+\boldsymbol{\lambda})\times \mathbf{s})_z & \epsilon_\pi \end{pmatrix}. \tag{13}$$

There are intrinsic SO linear in z_p and Rashba bilinear in $z_p \xi_{sy}$ interactions that contribute to the total SO interaction in the π structure. There is no correction for the kinetic interaction. The intrinsic SOC contribution between sites ι and $\jmath$ is given by

$$\mathcal{H}_{so}^{\iota\jmath} = i(\alpha_x s_y - \alpha_y s_x) = i(\boldsymbol{\alpha}\times \mathbf{s})_z, \tag{14}$$

where $\mathbf{s}$ is the vector of Pauli matrices and $\boldsymbol{\alpha}$ is the vector with the magnitude of the intrinsic SO in each coordinate that are defined as

$$\alpha_x = \frac{2 z_p V_x}{\epsilon_p}, \qquad \alpha_y = \frac{2 z_p V_y}{\epsilon_p}. \tag{15}$$

The estimated values, considering characteristic values for the oligopeptide, are $\alpha_x \sim 8.97$ meV and $\alpha_y \sim 10.20$ meV (see Appendix B). The Rashba SO has contributions from higher order terms from the Stark interaction in the form

$$\mathcal{H}_R^{\iota\jmath} = i(\lambda_x s_y - \lambda_y s_x) = i(\boldsymbol{\lambda}\times \mathbf{s})_z, \tag{16}$$

where $\boldsymbol{\lambda}$ is a vector with the Rashba SO magnitude in each component. They are given by

$$\begin{aligned} \lambda_x &= \frac{z_p(\xi_{\mathrm{sy},\iota} - \xi_{\mathrm{sy},\jmath})V_s}{\epsilon_{\mathrm{pz}}\epsilon_{\mathrm{s}}} - \frac{2 z_p \epsilon_{\mathrm{py}}^2 \epsilon_s \xi_{\mathrm{sx}}^2 V_x}{\epsilon_{\mathrm{px}}^2\left(\xi_{\mathrm{sy}}^2 - \epsilon_{\mathrm{py}}\epsilon_s\right)^2} \\ &\quad + \frac{2 z_p \xi_{\mathrm{sx}}\xi_{\mathrm{sy}} V_y}{\epsilon_{\mathrm{px}}\left(\xi_{\mathrm{sy}}^2 - \epsilon_{\mathrm{py}}\epsilon_s\right)}, \\ \lambda_y &= -\frac{2 i z_p \xi_{\mathrm{sy}}^2 V_y}{\epsilon_{\mathrm{py}}^2 \epsilon_s} + \frac{2 z_p \xi_{\mathrm{sx}}\xi_{\mathrm{sy}} V_x}{\epsilon_{\mathrm{px}}\left(\xi_{\mathrm{sy}}^2 - \epsilon_{\mathrm{py}}\epsilon_s\right)}. \end{aligned} \tag{17}$$

Note that the first-order contribution in Stark interaction on λ_x magnitude depends on the difference of the electric dipoles at two consecutive sites ι and $\jmath$, so even though this is the term of the highest order, it is not necessarily the largest in magnitude, therefore, we consider that the second order terms are important for this description. In fact, the estimated values for the largest contributions are $\lambda_x \sim 0.15$ meV and $\lambda_y \sim 1.2$ meV (see Appendix B), where we have considered that the angle of inclination of the hydrogen bonds with respect to the helix axis is very small, so ξ_{sx} is negligible against ξ_{sy}.

The full SO effective interaction can be written as, $\mathcal{H}_{SO} = \mathcal{H}_{so} + \mathcal{H}_R$. The properties of the system will be determined mainly by the lowest order terms of Eq. (13). However, in the case of mechanical deformations, higher order terms may be are relevant, so we consider here interactions up to second order in ξ_{sy} and first order in ξ_{sx}. Then, the spin interactions of the effective Hamiltonian are determined mostly by the intrinsic SO, and the Rashba contribution become of comparable size in the case of mechanical deformations.

III. BLOCH SPACE HAMILTONIAN

Consider a local cartesian coordinate system that is on top of an atom, then each atom on the chain will have the same system. The nearest neighbor atoms are described by the following vectors in the local system:

$$\mathbf{r}' = \sqrt{2} r \mathbf{e}_x + \frac{h}{4}\mathbf{e}_y. \tag{18}$$

Considering only first nearest neighbors interaction, the Hamiltonian can be taken as the Bloch sum of matrix elements. Considering $k_z = 0$ and assuming that the contribution of each site is independent with nearest neighbor interaction only, the Bloch expansion can be obtained as

$$\begin{aligned} \mathcal{H}(k) &= \frac{1}{N}\sum_{\iota=1}^{N}\sum_{\jmath=1}^{N} e^{i\mathbf{k}\cdot\mathbf{R}_{\iota\jmath}} \langle\phi_\iota|\mathcal{H}|\phi_\jmath\rangle \\ &= \frac{1}{N}\sum_{\iota=1}^{N}\left(\sum_{\jmath=\iota}\langle\phi_\iota|\mathcal{H}|\phi_\iota\rangle + \sum_{\jmath\neq\iota} e^{i\mathbf{k}\cdot\mathbf{R}_{\iota\jmath}}\langle\phi_\iota|\mathcal{H}|\phi_\jmath\rangle\right) \\ &= \frac{1}{N}\sum_{\iota=1}^{N}(\epsilon_\pi \mathbf{1}_s + V_z f(\mathbf{k})\mathbf{1}_s + g(\mathbf{k})((\boldsymbol{\alpha}+\boldsymbol{\lambda})\times\mathbf{s})_z) \\ &= \epsilon_\pi \mathbf{1}_s + V_z f(\mathbf{k})\mathbf{1}_s + g(\mathbf{k})((\boldsymbol{\alpha}+\boldsymbol{\lambda})\times\mathbf{s})_z, \end{aligned} \tag{19}$$

where we have only taken nearest neighbor couplings and strict periodicity of the lattice turn by turn. In Eq. (19), ϕ_ι are the orbitals per unit cell and N is the number of the unit cells in the molecule. This model considers an approximate structure, shown in Fig. 1(a), where the angle, $\Delta\phi$, between successive aminoacids is smaller than the angle for real oligopeptides [22]. The latter assumption is not quite correct for oligopeptides since there is a small incommensurability (non-periodicity in the axial direction) of the potential when one goes from one turn to the next. This is an approximation of the model .

The helix can be considered as a one-dimensional (1D) system in the local frame that satisfies $\tan\eta = h/2\pi r$. Then, the k functions in Eq. (19) are

$$f(\mathbf{k}) = \cos(\mathbf{k}\cdot\mathbf{r}'), \quad g(\mathbf{k}) = \sin(\mathbf{k}\cdot\mathbf{r}'). \tag{20}$$

The spectra of the system can be obtained by solving the secular equation

$$\det(\mathcal{H}(k) - E\mathbf{S}) = 0, \tag{21}$$

where **S** is the overlap matrix and we assume that the eigenfunctions are orthogonals, such that $S = 1$. By solving the full system, Eq. (21), we obtain the spectra of the system for the two spin species, and is given by

$$E_{\pm}(k) = V_z \cos(\mathbf{k}\cdot\mathbf{r}') \pm |\boldsymbol{\alpha} + \boldsymbol{\lambda}| \sin(\mathbf{k}\cdot\mathbf{r}'), \tag{22}$$

where each band correspond to a different spin species.

A. Hamiltonian in vicinity of half filling

We consider the orbitals that provide mobile electrons, to be half filled as a reference, when the molecule is isolated. However, deviation from half filling occurs due to electron doping by the molecular environment, e.g., the residues of the amino acid are projected into the water phase, resulting in the polarization of the molecular unit adding/withdrawing electrons from the carbonyl group [35]. Consider that the Fermi energy of p_z orbital is $\epsilon_F = 0$. By solving Eq. (21) only for the kinetic component at half filling, $\epsilon_F = V_z \cos(k_F R) = 0$, the Fermi vector is $k_F = \pi/2R$, where $R = \sqrt{2}r + \tan\eta h/4$. To describe the physics in the vicinity of the Fermi level, consider a small perturbation q around k_F, such that $k = k_F - |\mathbf{q}|$, and $|\mathbf{q}|R < 1$. Then, the Bloch expansion of the system, Eq. (19) can be approximated as

$$\mathcal{H}_{1/2}(q) = \epsilon_\pi + V_z qR + ((\boldsymbol{\alpha} + \boldsymbol{\lambda}) \times \mathbf{s})_z. \tag{23}$$

The spectra of the system shows that the bands do not cross each other, they are always separated by a constant gap between spin up and spin down states of the order of $|\alpha| \sim 10^{-2}$ eV. In such a system, the SO interaction is not coupled to momentum in the vicinity of k_F. Nevertheless, molecular contact with an environment, either a surface or surrounding structure will dope the system due to difference in electronegativity. We must then consider an energy shift by above or below $\epsilon_F = 0$. One can expand Eq. (19) around the doped energy, and the resulting expression has a spin component linear in momentum. Let us consider a small deviation from k_F, that is, $k' = 3\pi/5R$. The effective Hamiltonian around k' is

$$\mathcal{H}_{k'}(q) = \epsilon_\pi + V_z\left(\frac{1-\sqrt{5}}{4} - \sqrt{\frac{5+\sqrt{5}}{8}}qR\right) + ((\boldsymbol{\alpha} + \boldsymbol{\lambda}) \times \mathbf{s})_z\left(\frac{1-\sqrt{5}}{4}qR + \sqrt{\frac{5+\sqrt{5}}{8}}\right). \tag{24}$$

Coupling between momentum and spin causes wave functions with a chiral component that increases approaching a crossing point at $k = 0$.

The previous Hamiltonian, aside from the geometrical details that determine the SO strength to within tens of meV, has the same form as that of DNA [15] and of helicene [16] and leads to polarized electron transport, as has been reported experimentally [4,17].

IV. SPIN ACTIVE DEFORMATION POTENTIALS

In this section we show the behavior, under mechanical deformations, of the SOC magnitudes. The response to deformations depends on the geometrical relations of the orbitals involved and will serve to provide an experimental probe to the model [17]. Although DNA and oligopeptides are helices, the orbitals involved are quite different and thus should be distinguishable in a mechanical probe.

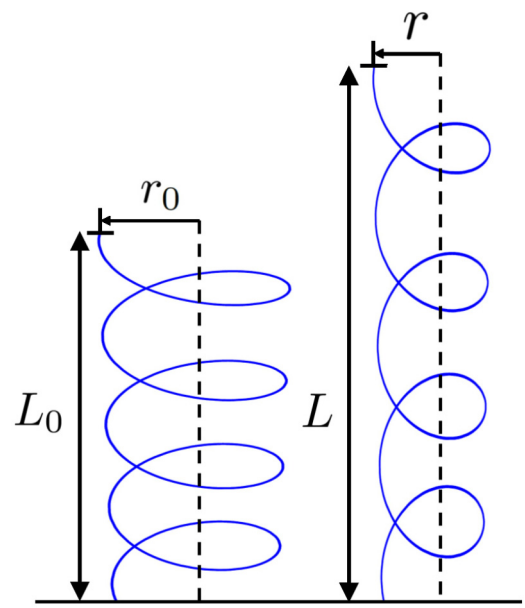

FIG. 2. Graphical representation of a mechanical deformation setup. Left: Oligopeptide in initial structure r_0 and L_0. Right: Stretched structure along the helical axis to r and L.

We consider stretching and/or compressing of the oligopeptide model in the form shown in the schematic Fig. 2. In the deformation scheme, we consider that the rotation angle $\Delta\varphi$ (see Fig. 1) between consecutive atoms does not change for small deformations. The longitudinal strain is defined as $\varepsilon = (L - L_0)/L_0$ where L_0 and L are the initial and final lengths of the helix, respectively. A change in ε implies a change on the radius and pitch, such that $r = r_0(1 - \nu\varepsilon)$ and $h = h_0(1 + \varepsilon)$, where ν is the Poisson ratio of the helix [36,37]. For our model, the Poisson ratio was taken from experimental data in Ref. [38]. The deformation changes the relative distances between orbitals, so the magnitude of the vector connecting two neighboring sites is written in the form

$$R_{jl}(\varepsilon) = \sqrt{r_0^2(1-\nu\varepsilon)^2 + h_0^2(1+\varepsilon)^2/16}. \tag{25}$$

The expressions for the SO intrinsic terms are

$$\alpha_x = \frac{2\hbar^2 z_p}{m\epsilon_p (R_{jl}(\varepsilon))^2}\left(\kappa_{pp}^{\pi} - \frac{r_0^2(1-\nu\varepsilon)^2(\kappa_{pp}^{\sigma} - \kappa_{pp}^{\pi})}{(R_{jl}(\varepsilon))^2}\right), \tag{26}$$

and

$$\alpha_y = -\frac{2\hbar^2 z_p r_0 h_0 (1-\nu\varepsilon)(1+\varepsilon)(\kappa_{pp}^{\sigma} - \kappa_{pp}^{\pi})}{m\epsilon_p (R_{jl}(\varepsilon))^4}, \tag{27}$$

where we have considered that $\epsilon_p^{\pi} = \epsilon_p^{\sigma} = \epsilon_p$, and $\kappa_{pp}^{\pi\sigma}$ are the atomic parameters used in the Harrison formula [28] (see Appendices B and A for the equation and for the values of the parameters). For the first order dependence on ε we have

$$\alpha_x \approx \alpha_x^{(\varepsilon=0)} - 16 r_0 z_p C \nu \left(\kappa_{pp}^{\sigma} - \kappa_{pp}^{\pi}\right)\varepsilon + \cdots, \tag{28}$$

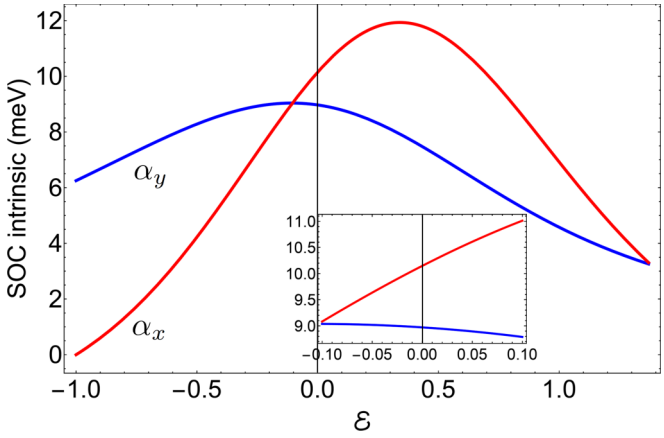

FIG. 3. SOC intrinsic intensities α_x and α_y versus deformation ε. We used $r_0 = 0.23$ nm, $h_0 = 0.54$ nm, $\Delta\varphi = \pi/2$, and $\nu = 0.5$. For $\varepsilon = 0$, the intensity of the interactions are $\alpha_x = 8.97$ meV and $\alpha_y = 10.20$ meV.

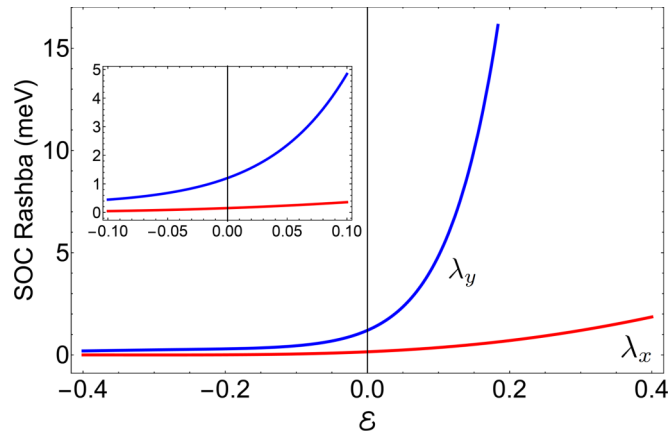

FIG. 4. Rashba magnitudes λ_x and λ_y versus deformation ε. We used $r_0 = 0.23$ nm, $h_0 = 0.54$ nm, $\Delta\varphi = \pi/2$, and $\nu = 0.5$. For $\varepsilon = 0$, the intensity of the interactions are $\lambda_x = 0.15$ meV and $\lambda_y = 1.2$ meV. Stretching the helix ($\varepsilon > 0$) increases the Rashba coupling while compressing decreases it.

and

$$\alpha_y \approx \alpha_y^{(\varepsilon=0)} + 8h_0 z_p C(1-\nu)\left(\kappa_{pp}^{\sigma} - \kappa_{pp}^{\pi}\right)\varepsilon + \cdots, \tag{29}$$

where we have defined the constant

$$C = \frac{64\hbar^2 r_0}{m\epsilon_p\left(h_0^2 + 16r_0^2\right)^2}.$$

The coefficients of the linear in ε are the spin-dependent *deformation potentials* [39] for the intrinsic interaction.

Figure 3 displays the intrinsic SOC magnitudes as a function of the deformation ε. Positive values for ε show the behavior when the helix is stretched and negative values when it is compressed. For small values of deformations, α_x grows with elongation at the same time as α_y slightly decreases (see inset in Fig. 3). However, the longitudinal deformation that arises from considering the SO net magnitude, has an increase during stretching and a decrease when compressed, the *opposite* behavior of the corresponding deformation configurations obtained for DNA [19].

The α_y increase reaches a maximum for an optimal strain value, in this case up to 20 meV, for a deformation of 20% with respect to the initial length. Thus, the magnitude of the interaction doubles with respect to the value without deformation. Nevertheless, this elongation may alter the assumed structure as hydrogen bonding may rupture [36].

The expressions for the Rashba terms as a function of deformation are

$$\lambda_x = \frac{\hbar^2 z_p \kappa_{sp}^{\sigma} r_0 (1-\nu\varepsilon)(\xi_{sy,\imath}(\varepsilon) - \xi_{sy,\jmath}(\varepsilon))}{m\epsilon_p \epsilon_s (R_{\jmath\imath}(\varepsilon))^3}, \tag{30}$$

and

$$\lambda_y = \frac{2\hbar^2 z_p (\xi_{sy}(\varepsilon))^2 r_0 h_0 (1-\nu\varepsilon)(1+\varepsilon)\left(\kappa_{pp}^{\sigma} - \kappa_{pp}^{\pi}\right)}{m\epsilon_s \epsilon_p^2 (R_{\jmath\imath}(\varepsilon))^4}, \tag{31}$$

where we only consider the first terms in Eq. (17) for λ_x and λ_y, since they are the most significant in magnitude. The Stark parameters are modulated by the changes in the polarization for a hydrogen bond due to the longitudinal deformation, in the same form that is in the recent work of Ref. [24]. They simulated in detail what happens to the near field electric field as a function of the O-H bonding distance. In Ref. [19], these changes in polarization where proposed to modulate a Rashba interaction on the double bonded atoms of the bases of DNA where these hydrogen bonds are attached. In oligopeptides, the origin of the SOC is the same but the hydrogen bond geometry is different yielding a contrasting mechanical response of the spin-active interaction.

The Rashba terms are proportional to the electric fields of the dipoles, therefore, when stretching the helix the relative distances between the orbitals become large, which decreases the Slater-Koster elements, but the length of the dipoles increase and this behavior is dominant such that it increases the Rashba magnitude, as it is shown in Fig. 4. This is the opposite behavior seen for DNA [19].

For the first order dependence of the Rashba interaction on ε we have

$$\lambda_x \approx \lambda_x^{(\varepsilon=0)} + \frac{\kappa_{sp} z_p C \nu (\xi_{sy,\imath} - \xi_{sy,\jmath})}{\epsilon_s \left(h_0^2 + 16r_0^2\right)^{-1/2}}\varepsilon + \cdots, \tag{32}$$

and

$$\lambda_y \approx \lambda_y^{(\varepsilon=0)} + \frac{8h_0 z_p C(1-\nu)(\xi_{sp})^2\left(\kappa_{pp}^{\pi} - \kappa_{pp}^{\sigma}\right)}{\epsilon_s \epsilon_p}\varepsilon + \cdots, \tag{33}$$

where the linear in ε terms are the spin-dependent deformation potentials of the Rashba coupling. Note that λ_x is sensitive to differences in the Stark interaction at two different sites. On the other hand, λ_y depends on the square of the Stark interaction. Although these features may lead to a smaller size of the SOC they are actually enhanced by deformation to be comparable to the intrinsic contribution (see Fig. 4).

In the deformation range of 10%, the magnitude of the Rashba interaction can increase up to five times its initial value (inset, Fig. 4). This result is opposite to the corresponding deformation previously obtained in the DNA, where stretching the helix longitudinally decreased the polarization of the hydrogen bonds that in that case were oriented transversely to deformation.

The behavior under deformation agrees qualitatively with that found in experiments [17], where spin polarization decreases with compression of the oligopeptide under an applied force. This experimental response to compressions of is qualitatively the same shown in Figs. 3 and 4, where a net decrease in the magnitude of the spin orbit coupling is observed, assuming there is a proportionality between the SOC magnitude and the respective polarization of spin. It is important to highlight that the quadratic terms in λ_y are much more sensitive to deformation than the first order term (λ_x), so deformations during experimental tests can induce higher order terms in interactions to contribute significantly to the magnitude of the effective coupling.

It is important to note that we consider a completely periodic model for the oligopeptide, however, an actual molecule does not repeat the sequence turn by turn, there being a small shift or incommensurability [22]. This non-periodicity can have two main effects on the behavior of the system: (a) the first is that the magnitude of the SK elements corresponding to the overlaps of the orbitals vary, since the angle $\Delta\varphi$ (see Fig. 1) between consecutive sites changes, impacting the magnitude of the SOC. This effect should be small; (b) the second effect is on the hydrogen bonding. The real molecule can have hydrogen bonds with small differences in their orientations with respect to the axis of the molecule. Although we have not accommodated for the geometrical effect we have captured the tilting of the bonds by introducing the two components of the electric dipoles through the Stark terms that give rise to the Rashba SOC, Eq. (32).

V. SUMMARY AND CONCLUSIONS

In this work we have studied a model for spin interactions in oligopeptides, paying particular attention to the peculiar hydrogen bonding producing the source electric fields for the SOC. We built a minimal analytic tight-binding model to describe the mobile electrons of the system in a helical geometry using the Slater-Koster approach. We assume mobile electrons spring from carboxyl group double bonds attached to amine groups directly in the near field electric field of polarized hydrogen bonding. Perturbative band folding then yields effective SO interactions of the intrinsic and Rashba types. We find a rich interplay between intrinsic and Rashba SOCs that allows manipulation of the spin polarization of oligopeptides under mechanical longitudinal deformation probes. The low-energy effective Hamiltonian, in the vicinity of the half filling Fermi level, shows the same form of Hamiltonians derived for DNA and Helicene that have shown spin polarization, explaining features of the CISS effect. The response to deformations expressed as spin-dependent deformation potentials, are consistent with the results of Ref. [17] and show opposite trends to the results previously found for DNA [19]. These results both make strong predictions to verify our orbital model and open the possibility of mechanical probes to spintronic properties of biological molecules. Hydrogen bonding as the source of spin activity further enhances (beyond chirality) the possible ubiquity of spin effects in biological systems, which coupled to tunneling effects [12], may be pervasive in many unexplored contexts.

TABLE III. Left column: SK parameters for s and p orbitals from [15]. Center column: Atomic parameters for carbon atoms from [15,26]. Right column: Structural parameters used to describe the oligopeptide [22]. In realistic systems, $\Delta\phi$ is different that $\pi/2$, but this value is used to have a commensurable system.

Parameter	eV	Parameter	eV	Parameter	Å/rad.
κ^{σ}_{pp}	−0.81	ϵ_p	−8.97	r	2.3
κ^{π}_{pp}	3.24	ϵ_s	−17.52	h	5.4
κ_{sp}	1.84	z_p	0.006	$\Delta\varphi$	$\pi/2$

ACKNOWLEDGMENTS

This work was supported by CEPRA VIII Grant No. XII-2108-06 "Mechanical Spectroscopy".

APPENDIX A: PARAMETERS FOR THE EFFECTIVE SYSTEM

We estimate the overlaps of the atomic wave functions using the empirical model described in Ref. [28]. The geometrical structure of the oligopeptide includes four atoms per turn and it does not differ significantly from realistic situations where oligopeptides are not strictly periodic from one turn to the next [22]. Atomic and structural parameters for the system are given in Table III. The SK and SO effective magnitudes are written in Table IV.

APPENDIX B: SLATER-KOSTER INTEGRALS

The overlap $E^{\iota\jmath}_{\mu\mu'}$ between orbitals μ and μ' that correspond to the site ι and $\jmath$, respectively, can be obtained using the expression [15,16]

$$E^{\iota\jmath}_{\mu\mu'} = \langle\mu_\iota|V|\mu'_\jmath\rangle = (\mathbf{n}(\mu_\iota), \mathbf{n}(\mu'_\jmath))V^{\pi}_{\mu\mu'} + \frac{(\mathbf{n}(\mu_\iota), \mathbf{R}_{\jmath\iota})(\mathbf{n}(\mu'_\jmath), \mathbf{R}_{\jmath\iota})}{(\mathbf{R}_{\jmath\iota}, \mathbf{R}_{\jmath\iota})}(V^{\sigma}_{\mu\mu'} - V^{\pi}_{\mu\mu'}), \quad \text{(B1)}$$

where $\mathbf{n}(\mu_\jmath)$ is the unit vector on the direction of the orbital μ of site $\jmath$, $\mathbf{R}_{\jmath\iota}$ is the vector that connect two consecutive sites, and $V^{\sigma}_{\mu\mu'}$ and $V^{\pi}_{\mu\mu'}$ represent the SK overlaps of the orbitals.

The unit vector of each orbital in a local coordinate system (xyz) on site ι is given by

$$\begin{aligned}
\hat{\mathbf{n}}(s_\iota) &= \hat{\mathbf{R}}_{\jmath\iota},\\
\hat{\mathbf{n}}(x_\iota) &= -\sin(\varphi_\iota)\mathbf{e}_x + \cos(\varphi_\iota)\mathbf{e}_z,\\
\hat{\mathbf{n}}(y_\iota) &= \mathbf{e}_y,\\
\hat{\mathbf{n}}(z_\iota) &= \cos(\varphi_\iota)\mathbf{e}_x + \sin(\varphi_\iota)\mathbf{e}_z. \quad \text{(B2)}
\end{aligned}$$

TABLE IV. Estimation of effective interactions for the system without deformations. Left column: Hopping interactions. Right column: SO interactions.

Parameter	eV	Parameter	meV
V_s	3.786	α_x	8.97
V_x	−4.143	α_y	10.20
V_y	−7.666	λ_x	0.15
V_z	−3.265	λ_y	1.2

The SK terms have a dependence on the distance representing in the empirical expression in the literature [28]

$$V^{\pi,\sigma}_{\mu\mu'} = \kappa^{\pi,\sigma}_{\mu\mu'}\frac{\hbar^2}{mR^2_{J\imath}}, \tag{B3}$$

where m is the mass of the electron and $\kappa^{\pi,\sigma}_{\mu\mu'}$ depend on the specific set of orbitals or atoms.

Without loss of generality we can assume that $E^{\imath J}_{\mu\mu'} = 0$, where $\mu = \{s, p_x, p_y\}$, because those electrons form the bond. The SK integrals that are relevant for transport processes, in terms of general parameters of the structure, are the following:

$$\begin{aligned}
E^{\imath J}_{zz} &= \langle z_\imath|V|z_J\rangle \\
&= \cos[\Delta\varphi]V^{\pi}_{pp} - \frac{r^2}{|\mathbf{R}_{J\imath}|^2}(1-\cos[\Delta\varphi])^2\big(V^{\sigma}_{pp} - V^{\pi}_{pp}\big), \\
E^{\imath J}_{zx} &= \langle z_\imath|V|x_J\rangle \\
&= \sin[\Delta\varphi]\left(V^{\pi}_{pp} - \frac{r^2}{|\mathbf{R}_{J\imath}|^2}(1-\cos[\Delta\varphi])\big(V^{\sigma}_{pp} - V^{\pi}_{pp}\big)\right), \\
E^{\imath J}_{zy} &= \langle z_\imath|V|y_J\rangle \\
&= -\frac{hr}{|\mathbf{R}_{J\imath}|^2}(1-\cos[\Delta\varphi])(J-\imath)\big(V^{\sigma}_{pp} - V^{\pi}_{pp}\big) \\
E^{\imath J}_{zs} &= \langle z_\imath|V|s_J\rangle = \frac{r(1-\cos[\Delta\varphi])}{|\mathbf{R}_{J\imath}|}V^{\sigma}_{sp}.
\end{aligned} \tag{B4}$$

Using the geometry shown in Fig. 1, i.e., $\Delta\phi = \pi/2$, the following symmetry relations are obtained:

$$\begin{aligned}
V_z &= E^{ij}_{zz} = E^{ji}_{zz} = -\frac{r^2}{|\mathbf{R_{ji}}|^2}\big(V^{\sigma}_{pp} - V^{\pi}_{pp}\big), \\
V_s &= E^{ij}_{zs} = E^{ji}_{zs} = E^{ij}_{sz} = E^{ji}_{sz} = \frac{r}{|\mathbf{R}_{ji}|}V^{\sigma}_{sp}, \\
V_x &= E^{ij}_{zx} = -E^{ji}_{zx} = -E^{ij}_{xz} = E^{ji}_{xz} = V^{\pi}_{pp} - \frac{r^2}{|\mathbf{R_{ji}}|^2}\big(V^{\sigma}_{pp} - V^{\pi}_{pp}\big), \\
V_y &= E^{ij}_{zy} = -E^{ji}_{zy} = -E^{ij}_{yz} = E^{ji}_{yz} = -\frac{rh}{|\mathbf{R_{ji}}|^2}\big(V^{\sigma}_{pp} - V^{\pi}_{pp}\big).
\end{aligned} \tag{B5}$$

APPENDIX C: DERIVATION OF THE BAND-FOLDING FORMULA

Let us consider a system with two kinds of eigenstates α and β, which are weakly coupled to each other. The secular equation, in matrix form, can be written as

$$\begin{pmatrix} H_{\alpha\alpha} & H_{\alpha\beta} \\ H^{\dagger}_{\alpha\beta} & H_{\beta\beta} \end{pmatrix}\begin{pmatrix} v_\alpha \\ v_\beta \end{pmatrix} = E\begin{pmatrix} v_\alpha \\ v_\beta \end{pmatrix}, \tag{C1}$$

where $H_{\alpha\alpha}$ and $H_{\beta\beta}$ are the Hamiltonian of each kind with corresponding eigenstates v_α and v_β, respectively, and $H_{\alpha\beta}$ is their coupling. It is easy to see that $v_\beta = (\mathbf{1}E - H_{\beta\beta})^{-1}H^{\dagger}_{\alpha\beta}v_\alpha$. Then, v_α can be expressed as

$$\Big(H_{\alpha\alpha} + H_{\alpha\beta}\big(\mathbf{1}E - H_{\beta\beta}\big)^{-1}H^{\dagger}_{\alpha\beta}\Big)v_\alpha = Ev_\alpha. \tag{C2}$$

Expanding $(\mathbf{1}E - H_{\beta\beta})^{-1}$ to first order in $H_{\beta\beta}$ and E, we find that

$$\left(H_{\alpha\alpha} - H_{\alpha\beta}\frac{1}{H_{\beta\beta}}H^{\dagger}_{\alpha\beta}\right)v_\alpha = SEv_\alpha, \tag{C3}$$

where $S = (1 + H_{\alpha\beta}(H^{-1}_{\beta\beta})^2H^{\dagger}_{\alpha\beta})$.

Then,

$$S^{-1/2}(H_{\alpha\alpha} - H_{\alpha\beta}(H_{\beta\beta})^{-1}H^{\dagger}_{\alpha\beta})S^{-1/2}\Phi = E\Phi, \tag{C4}$$

where $\Phi = S^{1/2}v_\alpha$. Considering first order in $H^{-1}_{\beta\beta}$, the expression for the effective Hamiltonian reduces to Eq. (12).

[1] Z. Xie, T. Markus, S. Cohen, Z. Vager, R. Gutierrez, and R. Naaman, Nano Lett. **11**, 4652 (2011).
[2] B. Göhler, V. Hamelbeck, T. Z. Markus, M. Kettner, G. F. Hanne, Z. Vager, R. Naaman, and H. Zacharias, Science **331**, 894 (2011).
[3] I. Carmeli, K. S. Kumar, O. Heifler, C. Carmeli, and R. Naaman, Angew. Chem. Int. Ed. Engl. **53**, 8953 (2014).
[4] A. C. Aragones *et al.*, Small **13**, 1602519 (2016).
[5] K. Ray, S. P. Ananthavel, D. H. Waldeck, and R. Naaman, Science **283**, 814 (1999).
[6] O. Ben Dor, S. Yochelis, S. P. Mathew, R. Naaman, and Y. Paltiel, Nat. Commun. **4**, 2256 (2013).
[7] S. Yeganeh, M. A. Ratner, E. Medina, and V. Mujica, J. Chem. Phys. **131**, 014707 (2009).
[8] E. Medina, F. Lopez, M. A. Ratner, and V. Mujica, Europhys. Lett. **99**, 17006 (2012).
[9] Ai-Min Guo and Q.-F. Sun, Proc. Nat. Acad. Sci. **111**, 11658 (2014).
[10] Xu Yang, C. H. van der Wal, and B. J. van Wees, Phys. Rev. B **99**, 024418 (2019).
[11] S. Varela, E. Medina, F. Lopez, and V. Mujica, J. Phys.: Condens. Matter **26**, 015008 (2016).
[12] S. Varela, I. Zambrano, B. Berche, V. Mujica, and E. Medina, Phys. Rev. B **101**, 241410(R) (2020).
[13] C. L. Kane and E. J. Mele, Phys. Rev. Lett. **95**, 226801 (2005).
[14] F. D. M. Haldane, Phys. Rev. Lett. **61**, 2015 (1988).
[15] S. Varela, V. Mujica, and E. Medina, Phys. Rev. B **93**, 155436 (2016).
[16] M. Geyer, R. Gutierrez, V. Mujica, and G. Cuniberti, J. Phys. Chem. C **44**, 27230 (2019).
[17] V. Kiran, S. Cohen, and R. Naaman, J. Chem. Phys. **146**, 092302 (2017).
[18] S. Varela, V. Mujica, and E. Medina, Chimia **72**, 411 (2018).
[19] S. Varela, B. Montañes, F. Lopez, B. Berche, B. Guillot, V. Mujica, and E. Medina, J. Chem. Phys. **151**, 125102 (2019).
[20] M. S. Zöllner, S. Varela, E. Medina, V. Mujica, and C. Herrmann, J. Chem. Theory Comput. **16**, 2914 (2020).
[21] A. Shah, B. Adhikari, S. Martic, A. Munir, S. Shahzad, K. Ahmad, and H.-B. Kraatz, Chem. Soc. Rev. **44**, 1015 (2015).

[22] L. Pauling, R. B. Corey, and H. R. Branson, PNAS **37**, 205 (1951).
[23] C. Liu, J. W. Ponder, and G. R. Marshall, Proteins **82**, 3043 (2014).
[24] Y. B. Ruiz-Blanco, Y. Almeida, C. M. Sotomayor-Torres, and Y. Garcia, PloS ONE **12**, e0185638 (2017).
[25] D. Huertas-Hernando, F. Guinea, and A. Brataas, Phys. Rev. B **74**, 155426 (2006).
[26] S. Konschuh, M. Gmitra, and J. Fabian, Phys. Rev. B **82**, 245412 (2010).
[27] D. J. Chadi, Phys. Rev. B **16**, 790 (1977).
[28] W. A. Harrison, *Electronic Structure and the Properties of Solids. The Physics of the Chemical Bond* (Dover, New York, 1989).
[29] P. Löwdin, J. Chem. Phys. **19**, 1396 (1951).
[30] P. Löwdin, J. Math. Phys. **3**, 1171 (1962).
[31] P. Löwdin, Phys. Rev. **139**, A357 (1965).
[32] T. Boykin, J. Math. Chem. **52**, 1599 (2014).
[33] L. L. Foldy and S. A. Wouthuysen, Phys. Rev. **78**, 29 (1950).
[34] E. McCann and M. Koshino, Rep. Prog. Phys. **76**, 056503 (2013).
[35] N. Sewald and H. D. Jakubke, *Peptides: Chemistry and Biology* (Wiley, New York, 2002).
[36] R. Rohs, C. Etchebest, and R. Lavery, Biophys. J. **76**, 2760 (1999).
[37] E. J. Leon, N. Verma, S. Zhang, D. A. Lauffenburger, and R. D. Kamm, J. Biomat. Sci. Pol. Edn. **9**, 297 (1998).
[38] S. K. Gupta, A. McEwan, and I. Lukacevic, Phys. Lett. A **380**, 207 (2016).
[39] R. Winkler, *Spin-Orbit Coupling Effects in Two-Dimensional Electron and Hole Systems*, Springer Tracts in Modern Physics (Springer, Berlin, 2003).